Extracting Geothermal Potential Areas in Ecuador Using Hydrogeochemical Data and Their Principal Component Analysis

Danilo Ibarra[1,2], Kotaro Yonezu[1], Akane Ito[1], Akira Imai[1]

[1]Department of Earth Resources Engineering, Faculty of Engineering, Kyushu University, 744 Motooka, Fukuoka 819-0395, Japan

[2] Asociación Geotérmica Ecuatoriana (AGE), Quito/Ecuador

pachoibarra332@gmail.com

Keywords: *Geothermal exploration, Geochemistry, Principal Component Analysis (PCA), Ecuador.*

ABSTRACT

This study advances geothermal exploration in Ecuador through the application of Principal Component Analysis (PCA) to both existing geochemical data from the literature and new samples collected from previously little or unstudied springs, such as El Hondón, Salvefaccha, Quilotoa, Salinas de Bolívar, and Santa Rosa de Mamanguy. Ecuador's geothermal potential is significant, with six major geothermal plays covering 49.2% of the national territory, particularly in the northern and southern Andes, and parts of the southwestern coast.

A dataset comprising 451 samples was analyzed, including temperature, pH, and major ions, allowing for a comprehensive characterization of the geothermal waters. Geochemical classification using ternary diagrams was employed to assess the geochemical behavior, followed by the application of PCA to identify key factors influencing geothermal potential. Reservoir temperatures were estimated in the range of 68 to 155 °C for Quilotoa, 66 to 171 °C for El Hondón, 75 to 233 °C for Salvefaccha, and 62 to 231 °C for Oyacachi using alkali geothermometers. These estimated temperatures highlight the suitability of these sites for future geothermal exploration, both for electricity generation and direct-use applications.

PCA results revealed that conservative ions (Cl^-, Na^+, K^+) and temperature are key factors in the variability of geothermal waters, and identified several sites, including Portovelo, Nangulví, and Chimborazo among others, in the high-interest quadrant of the biplot, suggesting the existence of high-temperature hydrothermal systems. These findings highlight promising areas for future geothermal exploration and development.

1. INTRODUCTION

Geothermal energy represents a promising and sustainable resource, crucial for mitigating the environmental impact of fossil fuels and climate change. However, identifying and assessing geothermal resources, particularly those hidden beneath the surface, remains a significant challenge. This is especially relevant in regions with substantial volcanic activity, such as Ecuador, where geothermal exploration is still in its early stages, despite initial exploration efforts dating back to 1979. Geochemical exploration helps address these challenges by analyzing the chemical makeup of thermal waters and gases to understand underground conditions, which is crucial for locating promising geothermal sites.

This study aims to advance geothermal exploration in Ecuador by applying Principal Component Analysis (PCA) to new geochemical data from thermal and cold springs. The chemical composition of these waters is analyzed, the results are compared with existing literature, and PCA is used to highlight key factors influencing geothermal potential. With a large-scale data collection, this approach seeks to enhance our understanding of Ecuador's geothermal resources and identify promising areas for future exploration.

The following sections will detail our methodology, present our findings, and discuss their implications for geothermal research in the region, thereby setting the stage for future exploration and development in the field.

2. STUDY AREA

Ecuador is distinguished by its significant geothermal potential, as evidenced by the identification of six major geothermal "plays" according to Beate et al., (2021) (Figure 1). These "plays" include: (1) Galapagos Spreading Center, (2) Galápagos Hot Spot, (3) Northern Andes Highlands, (4) Southern Andes Highlands, (5) Costa Forearc Basin, and (6) Oriente Foreland Basin. The geothermal favorability map of Ecuador, developed by Jara-Alvear et al., (2023) (Figure 1), provides a detailed assessment of the most promising areas for future exploration and development, categorizing the territory into six favorability levels: very low, low, medium, high, very high, and extremely high.

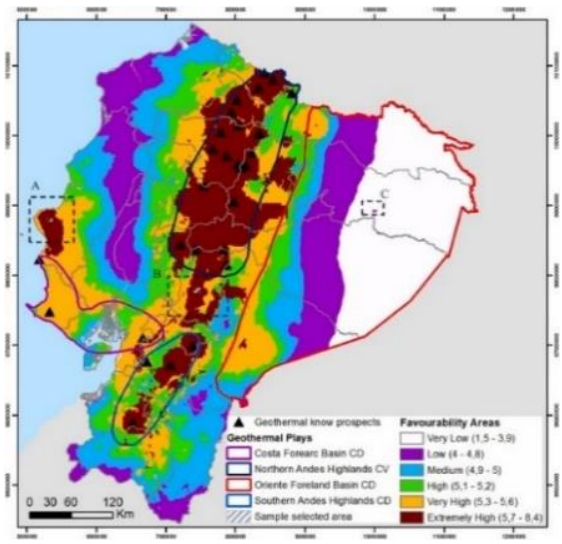

Figure 1: Map showing the favorability for a geothermal system presence in Ecuador (Jara-Alvear et al., 2023)

ISSN 2703-4275

Our study area focuses on regions with high to extremely high geothermal favorability, which cover approximately 49.2% of the national territory. These areas are primarily located along the northern Andes, in the southern Andes, in small areas of the southwestern coast, as well as in certain parts of the eastern region. These regions host 79% of the known geothermal prospects and are considered the most promising for future exploration. While northern Ecuador shows the highest identified geothermal potential, the southern Andes, and small areas of the coast and eastern region may harbor undiscovered geothermal resources, suggesting that the actual geothermal potential of the country may be significantly higher than current estimates. This extensive potential highlights the importance of concentrating our research in these high-favorability areas to maximize geothermal development opportunities.

3. METHODS

All diagrams and statistical tests were conducted using Python, a free and open-source software for statistical analysis and data visualization. The map was developed using QGIS, an open-source geographic information system software. Canva, an online graphic design tool, was used to add additional details to the diagrams for enhanced clarity and presentation.

3.1 Data compilation

Data were compiled from various published sources, including books, theses, conference papers, and journal articles, as well as unpublished sources like geochemical exploration reports and field notes from the authors, which are described later in the article. A total of 878 geothermal observation records, which include locations with surface manifestations related to geothermal resources or sites where samples were collected for geothermal, hydrological, or environmental studies, were gathered for interpretation. Some of these records included chemical data, while others simply described the presence of surface evidence. In Ecuador, geothermal drilling has only been conducted in Chachimbiro; however, no samples were obtained during the well tests, which limited the availability of subsurface data. Therefore, the compiled dataset relies on surface water sources such as rivers, cold and hot springs, and groundwater. The selection of nine variables—Temperature, pH, Na^+, K^+, Ca^{2+}, Mg^{2+}, Cl^-, SO_4^{2-}, and HCO_3^-—was based on their consistency across the dataset, as including other parameters like SiO_2 or isotopic data would have drastically reduced the number of available data points for interpretation.

3.2 Water sampling and analysis

After the literature review, springs with little or no chemical information were identified, leading to the collection of samples from 15 springs, including both hot and cold sources, between December 2023 and January 2024.

The sampling sites included the areas of El Hondón (2 samples), Oyacachi-Salvefaccha (6 samples), Salinas de Bolívar (5 samples), Quilotoa (1 sample), and Santa Rosa de Mamanguy (1 sample). Samples were collected in polyethylene bottles for major ion analysis. For cations, concentrated nitric acid was added as a preservative until the pH reached ≤ 2, ensuring stability during storage. In contrast, no preservative was used for anions. In situ measurements were taken for Temperature, Electrical conductivity (EC), pH, and HCO_3^-. Laboratory analysis for Na^+, K^+, Ca^{2+}, Mg^{2+}, Cl^- and SO_4^{2-} was conducted using ion chromatography at the Economic Geology Department of Kyushu University. The accuracy of major ion concentrations was verified by ion charge balance, with all samples falling within the acceptable range of ±5%, as recommended by (Domenico & Schwartz, 1998).

3.3 Statistical Analysis

The statistical analysis included calculating Pearson's correlation coefficients to assess the linear relationships between variables (Pearson, 1901). The nine variables, drawn from both literature and new data obtained as part of this study, were log-transformed to normalize different measurement scales and standardized to ensure equal contribution from all variables.

Principal Component Analysis (PCA) was performed to reduce the dimensionality of the dataset and identify the principal components (Giordani, 2018; Jolliffe, 2002). The PCA results were evaluated using a scree plot and cumulative variance analysis to determine the optimal number of components to retain. Detailed explanations and examples of PCA use, especially in the context of geochemistry and geothermal studies, can be found in the works of Golla (2018), Lindsey et al. (2018), Gao et al. (2019), Barzegar et al. (2020) and Jasnos (2021).

Finally, a biplot was created to visualize the two main principal components, illustrating relationships between samples and variables. This robust and accurate interpretation highlights significant patterns and relationships in the geochemical data.

4. RESULTS AND DISCUSSION

Reference samples from the Cerro Pabellón geothermal wells in Chile (Galarce, 2022) and Sol del Mañana in Bolivia (Villarroel, 2014) have been included in all the graphs. These samples, obtained from geothermal wells, are crucial for comparing the waters, validating the results, identifying patterns, differentiating groups, and facilitating reader understanding. Additionally, reference samples from the Chachimbiro geothermal system in Ecuador have also been included. Chachimbiro is the only geothermal prospect in Ecuador where a well has been drilled (1,987 m depth) and a bottom-hole temperature has been measured (235 °C) (Beate et al., 2023). However, since no reservoir fluid samples were obtained during the well tests, only the chemical information from cold and thermal springs has been used.

4.1 Hydrogeochemical Characteristics

After reviewing the literature, it was found that many geothermal observation records lacked complete or reliable geochemical data. In several cases, only the location and temperature were recorded, while in others, the geochemical information was partial or of poor quality. The geothermal observation records are detailed in (Aguilera et al., 2005; Almeida et al., 1992; Andrade & Palma, 2017; Betancourt & Guardado, 2019; Burbano et al., 2013; Carrera-Villacrés et al., 2016; Carrillo & Yandry, 2019; CELEC, 2012; CELEC EP, 2017; Changkuon et al., 1989; De Grys et al., 1970; González, 2003; Ibarra, 2018, 2022; Ibarra et al., 2015; INERHI, 1984; INER/SYR, 2014; Inguaggiato et al., 2010; Macas, 2019; Manrique-Carreño et al., 2023; Mariana et al., n.d.; Marini et al., 1991; Melian et al., 2021; Ruiz-Pico et al., 2019; SYR-Whistler-VRTON, 2015; Taussi et al., 2023). Following the exclusion of records with incomplete

ISSN 2703-4275

information and the verification of the ionic charge balance, ensuring that all samples fell within the acceptable range of ±5%, a total of 436 geothermal observation records with complete laboratory chemical data from the literature were selected for interpretation. This dataset was then complemented by 15 new samples collected in this study, resulting in a total of 451 samples available for interpretation. Hereafter, this set of 451 records will be referred to as "samples". The samples collected in this investigation are shown in Table 1. Additionally, as part of this study, it is intended to highlight locations with surface geothermal evidence that were excluded from interpretation to encourage their consideration for future geothermal exploration efforts. Examples of such sites include Chaucha, Peguche, and Jaramijó, whose locations are detailed in Figure 7.

Sample	Longitude	Latitude	Temp. [°C]	pH	Na [mg/L]	K [mg/L]	Ca [mg/L]	Mg [mg/L]	Cl [mg/L]	SO4 [mg/L]	HCO3 [mg/L]	Charge Balance (%)	Na/K Fournier 1979	Na/K Truesdell 1976	Na/K Giggenbach 1988	Na/K Tonani 1980	Na/K Nieva & Nieva 1987	Na/K Arnorsson 1983	K/Mg Giggenbach 1986
Quilotoa: AQ01	-78.87548	-0.85408	38.0	6.3	1862.0	59.8	465.3	332.1	3405.6	960.7	1525	-3.0	136	91	155	115	124	102	68
El Hondón: EH02	-77.91714	0.76271	84.0	7.8	1491.6	32.0	4.4	0.1	1449.3	408.0	1190	-2.4	113	66	133	87	102	77	171
El Hondón: EH09	-77.91730	0.76219	87.7	8.4	1416.3	31.3	4.3	5.2	1441.4	406.2	1037	-2.6	115	67	135	89	104	79	105
Oyacachi: OY06	-78.08825	-0.21571	42.2	8	978.6	21.5	219.7	77.0	769.3	115.2	1989	3.4	114	67	135	89	103	79	62
Oyacachi: OY01	-78.09126	-0.21523	35.5	7.9	933.8	91.7	95.9	65.4	793.2	201.2	1952	-4.4	215	186	231	221	202	193	99
Salvefaccha: 15/26	-78.16925	-0.22990	67.3	7.8	1075.5	98.6	3.2	0.1	1596.3	237.4	360	-4.5	210	178	225	213	197	186	219
Salvefaccha: SV03	-78.16362	-0.23013	42.2	5	308.4	19.9	157.6	19.9	305.5	84.3	854	-2.4	182	145	200	175	170	154	75
Salvefaccha: SV04/17	-78.16692	-0.22847	65.9	7.6	935.5	94.0	18.8	0.1	1462.7	158.1	311	-4.9	217	188	233	223	204	195	217
Salvefaccha: SV05/15	-78.16922	-0.22989	67.3	8	1095.1	106.1	8.0	0.1	1609.9	229.4	366	-3.7	214	184	230	219	201	192	222
S. de Bolívar: SB01	-79.03397	-1.40683	12.6	6.2	3162.0	406.3	290.9	69.2	4823.3	443.2	1281	1.1	239	216	253	255	226	222	144
S. de Bolívar: SB02	-79.03335	-1.40655	13.7	6.60	9963.0	1421.0	965.7	210.1	18025.0	1605.5	2501	-3.7	249	229	262	270	236	234	169
S. de Bolívar: SB06	-79.02700	-1.41810	13.7	6.2	6664.0	988.4	490.9	122.6	11736.4	662.4	1769	-2.7	253	234	266	276	239	239	166
S. de Bolívar: SB08	-79.01989	-1.40778	15.3	7.2	18096.0	2463.0	1292.2	350.6	31958.0	2006.0	4209	-2.9	245	223	258	263	231	229	181
S. de Bolívar: SB09	-79.02000	-1.40889	16.4	6.6	4374.0	644.6	375.1	80.0	7664.2	487.4	1525	-3.4	253	233	265	275	239	238	158

Table 1: Chemical composition of cold and thermal waters collected during this study

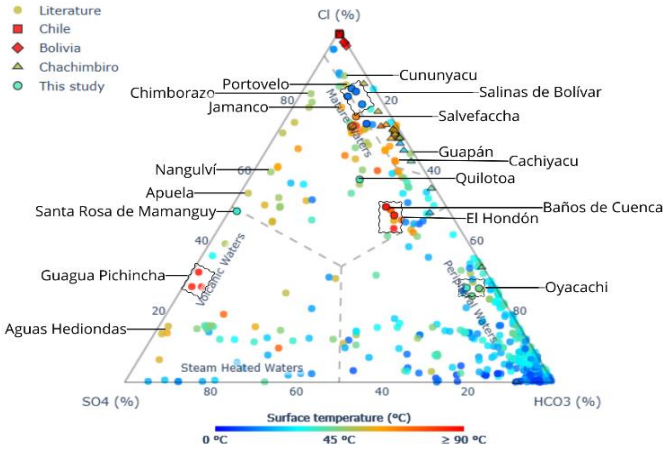

Figure 2: Cl–SO4–HCO3 ternary diagram

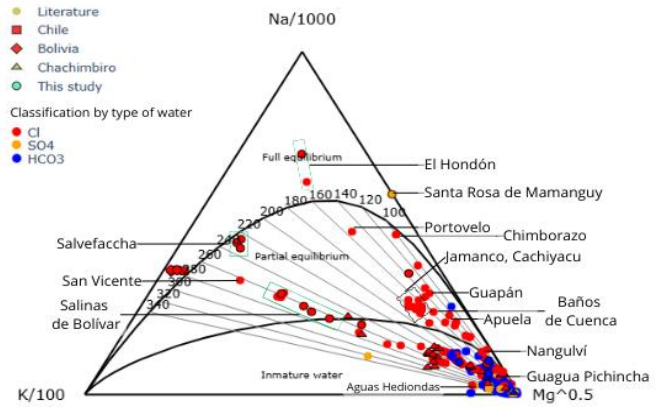

Figure 3: Na-K-Mg ternary diagram

Variables	PC1	PC2	PC3	PC4	PC5	PC6	PC7	PC8	PC9
Temperature	0.32	-0.22	0.35	0.33	-0.65	0.41	0.13	-0.12	-0.03
pH	-0.01	-0.85	-0.23	-0.39	0.08	0.08	0.12	-0.23	-0.01
Na^{+}	0.43	-0.16	0.02	0.11	0.18	-0.09	0.04	0.38	0.77
K^{+}	0.40	0.03	0.01	0.29	0.18	-0.51	0.18	-0.66	-0.04
Ca^{2+}	0.37	0.19	0.15	-0.21	0.47	0.60	-0.31	-0.28	-0.03
Mg^{2+}	0.28	0.36	-0.52	-0.30	-0.17	0.20	0.61	0.01	0.00
Cl^{-}	0.42	-0.18	0.10	0.11	0.27	-0.11	0.15	0.53	-0.62
SO_4^{2-}	0.29	0.11	0.34	-0.68	-0.35	-0.38	-0.23	0.02	-0.02
HCO_3^{-}	0.28	-0.04	-0.64	0.17	-0.27	-0.05	-0.63	0.04	-0.10
Eigenvalue	4.99	1.15	1.11	0.70	0.39	0.28	0.24	0.13	0.03
Variability (%)	55.34	12.71	12.36	7.73	4.28	3.13	2.68	1.46	0.32
Cumulative (%)	55.34	68.05	80.41	88.14	92.42	95.55	98.22	99.68	100.00

Table 2: Factor loading plots for different principal component

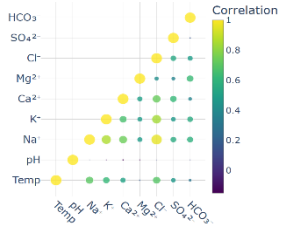

Figure 4: The correlation matrix based on Pearson's correlation coefficient

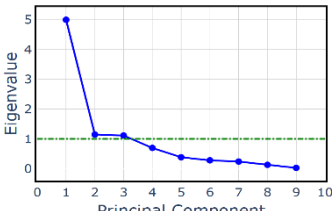

Figure 5: Scree Plot Showing Principal Components and Eigenvalues

From the 451 samples, the following physicochemical ranges were obtained. Temperatures varied between 6.0 and 88.4 °C, with pH values ranging from 2.50 to 9.50. Regarding ionic composition, Na^+ is predominant, with concentrations ranging from 1.15 to 21,710.01 mg/L, followed by Ca^{2+} with concentrations between 1.00 and 4,000 mg/L, K^+ ranging from 0.10 to 3,007.87 mg/L, and Mg^{2+} from 0.03 to 938 mg/L. Among the anions, Cl^- reaches up to 40,891 mg/L, SO_4^{2-} up to 4,540 mg/L, and HCO_3^- up to 4,209 mg/L.

4.2 Geochemical Classification of Analyzed Waters

The ternary Cl-SO_4-HCO_3 plot was employed to classify geothermal water samples and understand the geochemical processes within hydrothermal systems, as described by Giggenbach (1988) and Giggenbach & Goguel (1989). By analyzing the relative concentrations of chloride, sulfate, and bicarbonate, this plot distinguishes mature geothermal fluids, peripheral waters, and volcanic or steam-heated waters. It provides valuable insights into processes such as mixing, boiling, and fluid-rock interactions, which aid in interpreting the hydrogeochemical evolution of thermal waters (Aiuppa et al., 2002, 2003).

The ternary classification based on chloride, sulfate, and bicarbonate content reveals distinct geochemical behaviors and mixing patterns across Ecuador (Figure 2). The hottest Cl-type waters are found at El Hondón, in the southern sector of the Tufiño-Chiles-Cerro Negro area, with a temperature of 88.4 °C (Ibarra, 2022), and at Baños de Cuenca, with recorded temperatures of 87 °C (De Grys et al., 1970). These waters are positioned at the boundary with HCO_3-type waters on the ternary diagram, indicating significant mixing with bicarbonate-rich waters. Within the mature waters zone, reference samples from Cerro Pabellón (Chile), Sol del Mañana (Bolivia), and Chachimbiro are observed, alongside samples from Portovelo, Guagua Pichincha, Salinas de Bolívar, Baños de Cuenca, Cunnunyacu, Guapán, Chacana-Jamanco, and Chacana-Cachiyacu. Outside the mature waters zone, but trending towards peripheral waters, are Yanayacu (Cañar), Yanayacu (La Troncal), Salinas de Bolívar, Quilotoa, Baños de Cuenca, Chachimbiro, Chacana-Jamanco, Chacana-Cachiyacu, Chacana-Salvefaccha, Buenavista (Manabí), San Antonio de Manú (Loja), and El Hondón. Additionally, samples from Chacana-Jamanco, Quilotoa, Buenavista (Manabí), Cunnunyacu, Chimborazo, Nangulví, Portovelo, and Apuela show a trend towards volcanic zones.

The hottest SO_4-type waters are represented by a sample from Guagua Pichincha, reaching 88.2 °C (Marini et al., 1991), situated in the volcanic waters zone. It is worth noting that the hydrothermal system at Guagua Pichincha may have been significantly altered following the 1999 eruption, and it is possible that these springs no longer exist. Other notable samples in the volcanic waters zone include those from Tufiño-Chiles-Cerro Negro, Santa Rosa de Mamanguy, Baños de Agua Santa, and Portovelo, while another group of samples, specifically from Tufiño-Chiles-Cerro Negro and Tungurahua, are found in the steam-heated waters zone.

The hottest HCO_3-type waters are represented by the Agapantos sample from Baños de Cuenca, with a temperature of 58.7 °C (INER/SYR, 2014), positioned at the boundary between HCO_3-type and Cl-type waters, suggesting a potential mixing process. Additionally, Balneario Oyacachi (Chacana Caldera) hosts warm HCO_3-type waters with a temperature of 46.5 °C (Inguaggiato et al., 2010). Other warm waters with a tendency towards SO_4-type characteristics include those from Atuchan, Baños de Cuenca, and Baños de Agua Santa.

4.3 Aqueous Geothermometers

The Na-K-Mg ternary diagram was used to assess the water-rock equilibrium and the maturity of thermal waters in the study area (Giggenbach, 1988). This diagram helps distinguish between equilibrium waters, partial equilibrium waters, and immature waters by evaluating the balance among sodium, potassium, and magnesium concentrations. When Cl-type water samples fall within the full equilibrium and/or partial equilibrium zones, they are considered reliable for estimating hydrothermal reservoir temperatures. This approach is seen in studies by (Lindsey et al., 2018; Gao et al., 2019; Barzegar et al., 2020; Jasnos, 2021).

In Figure 3, it is observed that Cl-type waters are distributed across the three zones of the diagram. Reference samples from Cerro Pabellón (Chile) and Sol del Mañana (Bolivia) fall in the full equilibrium zone, near the K apex, indicating temperatures between 280°C and 300°C. In contrast, other reference samples from Chachimbiro (Ecuador), also Cl-type waters, are located in the lower part of the partial equilibrium zone and the upper part of the immature water zone, showing temperatures between 240°C and 260°C.

Furthermore, Cl-type samples seem to follow two distinct trends. The first trend extends toward the K apex, suggesting the presence of high-temperature reservoirs (>200°C). Within this trend, Salvefaccha samples are found at the boundary between the partial equilibrium and full equilibrium zones, indicating temperatures between 220°C and 240°C. Moving toward the boundary with the immature water zone, samples from San Vicente y Salinas de Bolívar are distributed, suggesting temperatures around 260°C. The second trend extends toward the Na apex, indicating the presence of lower temperature reservoirs. In this group, within the full and partial equilibrium zones, El Hondón samples show temperatures around 160°C. Other samples in the partial equilibrium zone, heading toward the immature water zone, include those from Portovelo, Chimborazo, Chacana-Jamanco, Chacana-Cachiyacu, Guapán, Baños de Cuenca, Apuela, and Nangulví.

In the immature water zone, most of the samples—Cl, SO4, and HCO3 types—are distributed. As the samples move closer to the Mg apex, clear interpretations become more challenging due to mixing, boiling, and other processes affecting the water, making the estimated temperatures less reliable.

Additionally, temperatures were estimated using the Na/K and K/Mg alkali geothermometers for the samples collected in this study. Table 1shows the following temperature ranges: Quilotoa from 68°C to 155°C, El Hondón from 66°C to 171°C, Salvefaccha from 75°C to 233°C, Oyacachi from 62°C to 231°C, and Salinas from 144°C to 276°C. For Santa Rosa de Mamanguy, further considerations might be required; it is presented as a new site of interest, likely having a temperature similar to its surface discharge (35.2°C). The applicability of the geothermometers is discussed in detail in studies such as Santoyo & Díaz-González (2010), which provide insights into their effectiveness under various geothermal conditions.With this in mind, it is important to note that this study does not aim to present geochemical models but rather to contribute new information to motivate

geothermal exploration, assess the potential, and evaluate the feasibility of utilizing the resource.

4.4 Principal Component Analysis

The Pearson correlation coefficients (Figure 4) reveal several key relationships among the variables. There is a high positive correlation (above 80%) between Cl^- and Na^+, Cl^- and K^+, as well as between Na^+ and K^+. Moderate to strong correlations (50-80%) are also evident between HCO_3^- and Na^+, K^+, and Mg^{2+}; SO_4^{2-} and Na^+, Ca^{2+}, and Cl^-; Cl^- and Temperature and Ca^{2+}; Mg^{2+} and Ca^{2+}; Ca^{2+} and Temperature, Na^+, and K^+; K^+ and Temperature; and Na^+ and Temperature. In contrast, pH shows very low correlation with all other parameters, and similarly, the correlations between HCO_3^- and SO_4^{2-}, HCO_3^- and Temperature, and Temperature and Mg^{2+} are almost negligible, indicating a minimal influence of these variables on the concentrations of the main ions.

Figure 5 shows the principal components vs. eigenvalue, commonly referred to as a scree plot. Kaiser's rule (Kaiser, 1960) only retains PCs with variances or eigenvalues that exceed 1. The results indicate that three principal components (eigenvalue > 1) were obtained, explaining 80.41% of the total variance. Table 1 highlights that the first principal component explains 55.34% of the variance, while the second and third components explain 12.71% and 12.36% respectively. Key observations include the high influence of Na^+, Cl^-, and K^+ on PC1. pH has a unique and dominant contribution to PC2, indicating its significant role in differentiating the samples along this axis. In PC3, Mg^{2+}, HCO_3^-, Temperature and SO_4^{2-} play a key role, suggesting their association with processes such as water-rock interaction and temperature-driven geochemical evolution. The cumulative variance explained by these three principal components underscores their importance in capturing the majority of the data's variability.

In the biplot of the principal components (PC1 and PC3) presented in Figure 6, each ion's contribution to the variability of the samples is shown, allowing us to understand the influence of each element on their geochemical distribution. For this analysis, PC3 was selected because it captures key aspects of geochemical behavior, such as temperature and other indicators of water-rock interaction, which are essential for understanding the hydrothermal context. Although PC2 is dominated by pH, it does not provide significant differentiation in terms of high-temperature systems, whereas PC3 better captures geochemical evolution, cooling processes, and mixing.

The vectors for Cl^-, Na^+, K^+, SO_4^{2-}, Ca^{2+}, and Temperature are oriented toward the first quadrant, indicating a high correlation among these parameters. The samples from Chile and Bolivia, located in the first quadrant, originate from deep hydrothermal environments with mature geochemistry, characterized by high concentrations of conservative ions and alkali cations. The orientation of the temperature vector reinforces that these samples originate from high-temperature reservoirs.

On the other hand, the vectors for HCO_3^- and Mg^{2+} are projected towards the fourth quadrant, suggesting characteristics associated with meteoric interaction and mineral alteration processes, typical of cooler waters and discharge areas. The samples from Chachimbiro, distributed between the first and fourth quadrants, show mixed characteristics. Some resemble the high-temperature references, while others reflect cooling and mixing processes, suggesting that they could represent transition or discharge areas within the hydrothermal system.

In summary, the biplot clearly differentiate the high-temperature fluids from Chile and Bolivia from those of Chachimbiro, suggesting that the latter reflect a mixture with cooler waters typical of an outflow zone. This context is key to interpreting the locations of the new samples, analyzing how their positions within the biplot relate to the vectors of different geochemical parameters and what implications they have regarding the origin and evolution of these fluids.

The samples collected in the Chacana Caldera correspond to Salvefaccha and Oyacachi. Salvefaccha had no geochemical results published in the geothermal context, highlighting the importance of the data presented in this study. In the case of Oyacachi, one of the samples was collected at the local bathhouse—the most accessible site, with multiple previous geochemical analyses—while the rest came from surrounding, less-studied springs. The samples from Salvefaccha, located in the first quadrant of the biplot, show characteristics similar to those of Chile and Bolivia, with high temperature and concentrations of Cl^- and Na^+, indicating high-energy conditions. In contrast, the samples from Oyacachi, projected towards the fourth quadrant, are associated with HCO_3^- and Mg^{2+}, reflecting the influence of meteoric waters and processes of mixing and cooling, typical of hydrothermal discharge areas.

The samples from El Hondón, collected south of the Tufiño-Chiles-Cerro Negro geothermal prospect, are located in the first quadrant of the biplot, similar to the high-temperature references from Chile and Bolivia. This position suggests that the fluids from El Hondón present comparable hydrothermal characteristics, with high concentrations of Cl^- and Na^+ and elevated temperatures, indicating favorable geothermal conditions and an active system. These results represent the first geochemical data published for El Hondón, along with those from a water sample taken by us in 2022, which had not been disclosed until now. According to previous studies of the area, the geothermal reservoir of the Tufiño-Chiles prospect is estimated to have a temperature of approximately 230 °C, with an estimated potential of 138 MWe (Beate, 2010), which reinforces its potential for high-enthalpy applications in the area.

Las muestras de Salinas de Bolívar y Quilotoa se ubican en el cuarto cuadrante del biplot, mostrando una tendencia hacia los vectores HCO_3^- y Mg^{2+}, sugiriendo una influencia significativa de aguas más frías y procesos de mezcla típicos de zonas de descarga hidrotermal. La alta salinidad observada en ambos sitios puede estar asociada a procesos de concentración, posiblemente debidos a la evaporación (Inguaggiato et al., 2010). Cabe destacar que la mayoría de las muestras tomadas en estos sitios son nuevas.

The sample from Santa Rosa de Mamanguy is located in the second quadrant of the biplot, indicating that it does not align with the typical vectors of deep or high-temperature hydrothermal systems, such as Cl^-, Na^+, K^+, or temperature. Its position suggests that the waters do not present significant characteristics of high temperature or high concentrations of conservative ions. Since there is no evidence of active

ISSN 2703-4275

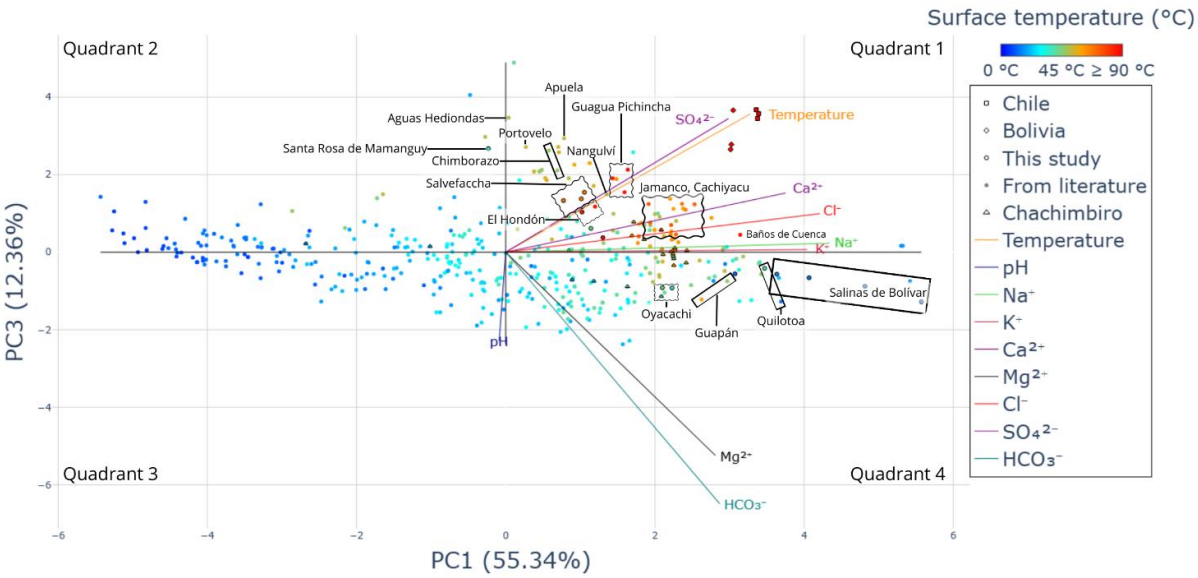

Figure 6: PCA bi-plot classified by surface temperature

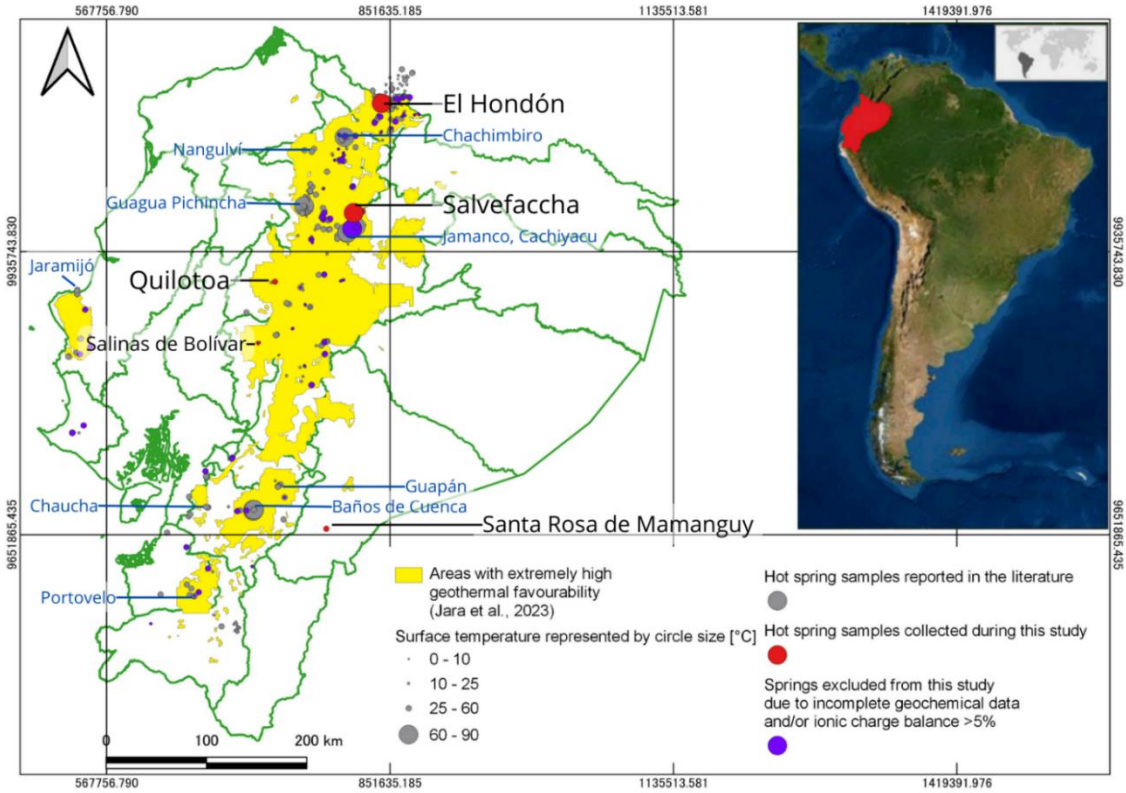

Figure 7: Map showing the location of hot springs in Ecuador

volcanism or significant geothermal information in the area, the sample could reflect a meteoric origin with possible tectonic influence. The presence of tectonic heat, generated by the friction of active faults, could explain the observed temperatures, suggesting a residual low-temperature system that could be suitable for local geothermal applications.

By applying principal component analysis and the biplot, other sites with characteristics similar to those of high-temperature reservoirs have been identified, highlighting the importance of these locations for future studies. In the first quadrant of the biplot, there are samples from less-studied sites such as Portovelo (E34), Apuela, Cununyacu (E28), and Nangulví, which show characteristics suggesting favorable geothermal conditions and require further analysis. Additionally, in this same quadrant, samples from sites that have been somewhat more investigated, such as Baños de Cuenca, Chacana Jamanco, and Chacana Cachiyacu, are also located, as shown in. These samples align with the vectors of high temperature and conservative ions, indicating the possible existence of deep and active hydrothermal systems in these areas. This analysis helps establish priorities for future explorations and assess the geothermal potential of these sites in the region.

2. CONCLUSION

This study advanced geothermal exploration in Ecuador through the collection and analysis of existing geochemical data from the literature, the collection of new samples from springs that were little or no studied (Figure 7), such as those from El Hondón, Salvefaccha, Quilotoa, Salinas de Bolívar, and Santa Rosa de Mamanguy, and the application of Principal Component Analysis (PCA), a technique that had not been previously applied in geochemical studies for geothermal exploration in the country. This allowed for a more comprehensive understanding of the geochemical composition of geothermal waters and advanced the identification of areas with favourable geothermal characteristics.

The 439 samples analyzed showed broad physicochemical ranges and diverse geochemical classifications, highlighting the predominance of Cl-type waters, which are distributed across different states of equilibrium according to the Cl-SO_4-HCO_3 and Na-K-Mg ternary diagrams. These diagrams allowed for the estimation of reservoir temperatures suitable for both electricity generation and direct uses. Specifically, temperatures in the range of 68 to 155 °C for Quilotoa, 66 to 171 °C for El Hondón, 75 to 233 °C for Salvefaccha, and 62 to 231 °C for Oyacachi were obtained using alkali geothermometers (Na/K and K/Mg).

The Principal Component Analysis (PCA) revealed key factors in the geochemistry of thermal waters, highlighting the significant impact of conservative ions (Cl^-, Na^+, K^+) and temperature on data variability. The PCA also showed that, among others, samples from sites such as Portovelo, Nangulví, and Chimborazo are located in the first quadrant of the biplot, the area of greatest interest, reflecting characteristics of high-temperature hydrothermal systems. This evidence highlights the potential of these areas and may motivate future exploration studies to assess their geothermal viability.

Overall, the results provide valuable information for prioritizing exploration in areas with high geothermal potential and significantly contribute to the understanding of geothermal resources. The application of PCA and the integration of new geochemical data make it possible to identify promising areas that should be considered in future geothermal research and development efforts.

ACKNOWLEDGEMENTS

We We acknowledge the financial support from JICA through the KIZUNA scholarship. Special thanks to Mami Mampuku, Rie Yamashiro, and Tatsuto Ino for their support. We also thank the Asociación Geotérmica Ecuatoriana (AGE) and the Instituto de Investigación Geológico y Energético (IIGE) for their assistance with logistics and fieldwork permits. Our sincere gratitude goes to Andrés Lloret, Danilo Asimbaya, and Freddy Trejo for their unconditional support in logistics, fieldwork, sample collection, and more.

REFERENCES

Aguilera, E., Cioni, R., Gherardi, F., Magro, G., Marini, L., & Pang, Z. (2005). Chemical and isotope characteristics of the Chachimbiro geothermal fluids (Ecuador). *Geothermics*, *34*(4), 495–517. https://doi.org/10.1016/j.geothermics.2005.04.004

Aiuppa, A., Bellomo, S., Brusca, L., D'Alessandro, W., & Federico, C. (2003). Natural and anthropogenic factors affecting groundwater quality of an active volcano (Mt. Etna, Italy). *Applied Geochemistry*, *18*(6), 863–882. https://doi.org/https://doi.org/10.1016/S0883-2927(02)00182-8

Almeida, E., Sandoval, G., Panichi, C., Noto, P., & Bellucci, L. (1992). *Modelo Geotérmico Preliminar de Areas Volcánicas del Ecuador, a partir de Estudios Químicos e Isotópicos de Manifestaciones Termales*.

Andrade, P., & Palma, A. (2017). *Caracterización geoquímica de las fuentes de agua de Tangalí para su uso potencial como recurso natural, Cantón Otavalo*. Universidad Técnica del Norte.

Barzegar, R., Asghari Moghaddam, A., Tziritis, E., Adamowski, J., Bou Nassar, J., Noori, M., Aalami, M. T., & Kazemian, N. (2020). Exploring the hydrogeochemical evolution of cold and thermal waters in the Sarein-Nir area, Iran using stable isotopes (δ18O and δD), geothermometry and multivariate statistical approaches. *Geothermics*, *85*, 101815. https://doi.org/https://doi.org/10.1016/j.geothermics.2020.101815

Beate, B. (2010). *Plan para el Aprovechamiento de los Recursos Geotérmicos en el Ecuador (in Spanish)*.

Beate, B., Urquizo, M., & Lloret, A. (2021). *Geothermal Country Update of Ecuador: 2015-2020*.

Beate, B., Urquizo, M., Lloret, A., Acosta, M., & Angulo, E. (2023). *Geothermal Country Update Ecuador 2020-2023*.

Betancourt, L., & Guardado, I. (2019). *Re-Evaluación del Potencial Geotérmico en el "Proyecto Geotérmico Chalpatán", Provincia del Carchi-Ecuador y Propuesta de Usos Directos para el Sector Rural*.

Burbano, N., Becerra, S., & Pasquel, E. (2013). *Aguas Termominerales en el Ecuador*.

Carrera-Villacrés, D., Guevara-García, P., & Delgado, V. (2016). *Hydrogeochemical analysis of volcanic and geothermal fluids in the Andes from Ecuador using hydrochemical plots (Stiff, Piper and Schoeller-Berkaloff diagrams)*.

Carrillo, R., & Yandry, F. (2019). *Caracterización hidroquímica de las aguas termales del sur del Ecuador*. Universidad Técnica Particular de Loja.

CELEC. (2012). *Consultoría para el Estudio de Prefactibilidad Inicial para Elaborar el Modelo Geotérmico Conceptual del Proyecto Chacana*.

CELEC EP. (2017). *Report on the Results of Thermal Samples from the Chachimbiro Geothermal Prospect*.

Changkuon, L., Aranyossy, J. F., Oleas, M., & Lopoukine, M. (1989). *Determinación del Modelo Geotérmico del Valle de los Chillos (Ecuador), en base a Isótopos Ambientales*.

De Grys, A., Vera, J., & Goossens, P. (1970). A note on the hot springs of Ecuador. *Geothermics*, *2*, 1400–1404. https://doi.org/10.1016/0375-6505(70)90457-8

Domenico, P. A., & Schwartz, F. W. (1998). *Physical and Chemical Hydrogeology* (2nd Edition). John Wiley & Sons Inc.

Galarce, F. (2022). *Modelamiento termodinámico de la alteración hidrotermal bajo condiciones de reservorio del sistema geotermal Cerro Pabellón, Cordillera de los Andes, Norte de Chile*. Universidad de Chile.

Gao, Z., Liu, J., Li, F., Wang, M., Feng, J., & Wu, G. (2019). Hydrochemical Characteristics and Temporal Variations of Geothermal Water Quality in Tangtou, Shandong, China. *Water*, *11*(8). https://doi.org/10.3390/w11081643

Giggenbach, W. F. (1988). *Geothermal solute equilibria. Derivation of Na-K-Mg-Ca geoindicators* (Vol. 52).

Giggenbach, W. F., & Goguel, R. L. (1989). *Collection and analysis of geothermal and volcanic water and gas discharges*.

Giordani, P. (2018). Principal Component Analysis. In R. Alhajj & J. Rokne (Eds.), *Encyclopedia of Social Network Analysis and Mining* (pp. 1831–1844). Springer New York. https://doi.org/10.1007/978-1-4939-7131-2_154

Golla, J. (2018). Using Principal Component Analysis to Aid in Visualization and Interpretation of Geothermal Solute Chemistry: An Application to Yellowstone Thermal Waters. *Transactions - Geothermal Resources Council*, *42*, 1226–1239.

González, M. (2003). *Caracterización Geotérmica y Consideraciones Ambientales de los Baños Termales de San Vicente, Provincia del Guayas*. Escuela Superior Politecnica del Litoral.

Ibarra, D. (2018). *Field Notes on the Chalupas Geothermal Prospect*.

Ibarra, D. (2022). *Report on the Results of Thermal Water from El Hondón*.

Ibarra, D., Mendoza, B., Asimbaya, D., Vaca, R., & Jimbo, G. (2015). *Caracterización Geoquímica e Hidrogeológica para el Aprovechamiento Geotérmico en la Provincia de Chimborazo*.

INERHI. (1984). *Inventario hidrotermal del Ecuador, primera investigación*.

INER/SYR. (2014). *Evaluación Preliminar del Sistema Geotermal de Baños de Cuenca*.

Inguaggiato, S., Hidalgo, S., Beate, B., & Bourquin, J. (2010). Geochemical and isotopic characterization of volcanic and geothermal fluids discharged from the Ecuadorian volcanic arc. *Geofluids*, *10*(4), 525–541. https://doi.org/10.1111/j.1468-8123.2010.00315.x

Jara-Alvear, J., De Wilde, T., Asimbaya, D., Urquizo, M., Ibarra, D., Graw, V., & Guzmán, P. (2023). Geothermal resource exploration in South America using an innovative GIS-based approach: A case study in Ecuador. *Journal of South American Earth Sciences*, *122*, 104156. https://doi.org/https://doi.org/10.1016/j.jsames.2022.104156

Jasnos, J. (2021). Hydrogeochemical Characteristics of Geothermal Waters from Mesozoic Formations in the Basement of the Central Part of the Carpathian Foredeep and the Carpathians (Poland) Using Multivariate Statistical Methods. *Energies*, *14*(13). https://doi.org/10.3390/en14134022

Jolliffe, I. T. (2002). *Principal Component Analysis*. Springer-Verlag.

Kaiser, H. F. (1960). The application of electronic computers to factor analysis. *Educational and Psychological Measurement*, *20*, 141–151.

Lindsey, C. R., Neupane, G., Spycher, N., Fairley, J. P., Dobson, P., Wood, T., McLing, T., & Conrad, M. (2018). Cluster analysis as a tool for evaluating the exploration potential of Known Geothermal Resource Areas. *Geothermics*, *72*, 358–370. https://doi.org/https://doi.org/10.1016/j.geothermics.2017.12.009

Macas, C. (2019). *Caracterización Hidroquímica de Surgencias y Aportantes Superficiales del Embalse Salvefaccha*. Universidad Internacional SEK.

Manrique-Carreño, J., Martínez-Villa, É., Calderón-Maza, É., & Guamán-Jaramillo, G. (2023). Geochemical characterization of Lithium-bearing brines from Guaranda, Ecuador. *Boletín de Geología*, *45*.

Mariana, L., Noroña, B., Del, I., & Guardado De Morán, R. (n.d.). *UNIVERSIDAD DE EL SALVADOR FACULTAD DE INGENIERÍA Y ARQUITECTURA ESCUELA DE POSGRADOS "PROYECTO GEOTÉRMICO CHALPATÁN", PROVINCIA DEL CARCHI-ECUADOR Y PROPUESTA DE USOS DIRECTOS PARA EL SECTOR RURAL. AUTORES.*

Marini, L., Agostini, A., Cioni, R., Guidi, M., & Leon, O. (1991). *Guagua Pichincha volcano , Ecuador : fluid geochemistry in volcanic surveillance*. *46*, 21–35.

Melian, G., Toulkeridis, T., Pérez, N., Hernández, P., Somoza, L., Padrón, E., Amonte, C., Alonso, M., Asensio-Ramos, M., & Cordero, M. (2021). Geochemistry of Water and Gas Emissions From Cuicocha and Quilotoa Volcanic Lakes, Ecuador. *Front. Earth Sci. 9:741528*.

Pearson, K. (1901). LIII. On lines and planes of closest fit to systems of points in space. *The London, Edinburgh, and Dublin Philosophical Magazine and Journal of Science*, *2*(11), 559–572. https://doi.org/10.1080/14786440109462720

Ruiz-Pico, Á., Pérez-Cuenca, Á., Serrano-Agila, R., Maza-Criollo, D., Leiva-Piedra, J., & Salazar-Campos, J. (2019). Hydrochemical characterization of groundwater in the Loja Basin (Ecuador). *Applied Geochemistry*, *104*, 1–9. https://doi.org/https://doi.org/10.1016/j.apgeochem.2019.02.008

Santoyo, E., & Díaz-González, L. (2010). A New Improved Proposal of the Na/K Geothermometer to Estimate Deep Equilibrium Temperatures and their Uncertainties in Geothermal Systems. In *Proceedings World Geothermal Congress*.

SYR-Whistler-VRTON. (2015). *Informe Geoquímico Parcial del Proyecto Geotérmico Binacional Tufiño-Chiles-Cerro Negro*.

Taussi, M., Tardani, D., Tassi, F., Gorini, A., Aguilera, E., Capaccioni, B., & Renzulli, A. (2023). A conceptual model for the Tufiño-Chiles-Cerro Negro (TCCN) geothermal system (Ecuador-Colombia): New insights into geothermal exploration from chemical and isotopic composition of hydrothermal fluids. *Journal of Geochemical Exploration*, *249*, 107214. https://doi.org/https://doi.org/10.1016/j.gexplo.2023.107214

Villarroel, D. (2014). *Geochemical studies of geothermal fluid and evaluation of well test results from wells SM-01, SM-02 and SM-03, Sol de Mañana field, geothermal project, Laguna Colorada Bolivia.*